# Phenotypic and pathomorphological characteristics of a novel mutant mouse model for maturity-onset diabetes of the young type 2 (MODY 2)

L. van Bürck, A. Blutke, S. Kautz, B. Rathkolb, M. Klaften, S. Wagner, E. Kemter, M. Hrabé de Angelis, E. Wolf, 4 B. Aigner, R. Wanke, and N. Herbach

<sup>1</sup>Institute of Veterinary Pathology, Center for Clinical Veterinary Medicine, and <sup>2</sup>Institute of Molecular Animal Breeding and Biotechnology, Department of Veterinary Sciences, LMU Munich, Munich; <sup>3</sup>Institute of Experimental Genetics, Helmholtz Zentrum München, Neuherberg; and <sup>4</sup>Laboratory for Functional Genome Analysis (LAFUGA), Gene Center, LMU Munich, Munich, Germany

Submitted 24 July 2009; accepted in final form 27 November 2009

van Bürck L, Blutke A, Kautz S, Rathkolb B, Klaften M, Wagner S, Kemter E, Hrabé de Angelis M, Wolf E, Aigner B, Wanke R, Herbach N. Phenotypic and pathomorphological characteristics of a novel mutant mouse model for maturity-onset diabetes of the young type 2 (MODY 2). Am J Physiol Endocrinol Metab 298: E512-E523, 2010. First published December 1, 2009; doi:10.1152/ajpendo.00465.2009.—Several mutant mouse models for human diseases such as diabetes mellitus have been generated in the large-scale Munich ENU (N-ethyl-N-nitrosourea) mouse mutagenesis project. The aim of this study was to identify the causal mutation of one of these strains and to characterize the resulting diabetic phenotype. Mutants exhibit a T to G transversion mutation at nt 629 in the glucokinase (Gck) gene, leading to an amino acid exchange from methionine to arginine at position 210. Adult Munich Gck<sup>M210R</sup> mutant mice demonstrated a significant reduction of hepatic glucokinase enzyme activity but equal glucokinase mRNA and protein abundances. While homozygous mutant mice exhibited growth retardation and died soon after birth in consequence of severe hyperglycemia, heterozygous mutant mice displayed only slightly elevated blood glucose levels, present from birth, with development of disturbed glucose tolerance and glucose-induced insulin secretion. Additionally, insulin sensitivity and fasting serum insulin levels were slightly reduced in male mutant mice from an age of 90 days onward. While \( \beta\)-cell mass was unaltered in neonate heterozygous and homozygous mutant mice, the total islet and  $\beta$ -cell volumes and the total volume of isolated β-cells were significantly decreased in 210-day-old male, but not female heterozygous mutant mice despite undetectable apoptosis. These findings indicate that reduced total islet and β-cell volumes of male mutants might emerge from disturbed postnatal islet neogenesis. Considering the lack of knowledge about the pathomorphology of maturity-onset diabetes of the young type 2 (MODY 2), this glucokinase mutant model of reduced total islet and total  $\beta$ -cell volume provides the opportunity to elucidate the impact of a defective glucokinase on development and maintenance of  $\beta$ -cell mass and its relevance in MODY 2 patients.

glucokinase;  $\beta\text{-cell};$  pancreas; Munich ENU mouse mutagenesis project

THE CATALYTIC ENZYME GLUCOKINASE is one of the four members of the hexokinase family, but its kinetics differs from those of the other hexokinases because of a lower affinity for glucose, the lack of physiologically relevant direct feedback inhibition by its product glucose-6-phosphate (G6P), and its sigmoidal kinetics (34, 35). Since glucokinase catalyzes the first, ratelimiting step of glycolysis—the phosphorylation of glucose to

Address for reprint requests and other correspondence: L. van Bürck, Inst. of Veterinary Pathology, Veterinärstr. 13, 80539 Munich, Germany (e-mail: vanbuerck@patho.vetmed.uni-muenchen.de).

G6P—it is considered a "glucose sensor." Mutations in the glucokinase gene (*GCK*) can cause hyperglycemia as well as hypoglycemia (19). Homozygous inactivating mutations in human *GCK* are associated with permanent neonatal diabetes mellitus (PNDM), whereas heterozygous inactivating mutations lead to maturity-onset diabetes of the young type 2 (MODY 2), a well-known specific form of diabetes (3, 22).

MODY, representing a genetically and clinically heterogeneous group of diabetes subtypes, is characterized by an autosomal dominant mode of inheritance (22), early onset of hyperglycemia due to defects in β-cell function, and disturbed insulin secretion, whereas insulin action usually is not impaired (3). In contrast to other MODY subtypes, like MODY 1 and 3 (61), MODY 2 is characterized by mild but chronic hyperglycemia, which may deteriorate little with age but usually remains considerably stable because of compensatory mechanisms such as, for instance, overexpression of the wild-type allele (22). Despite being present from birth, the diabetic phenotype often remains undiagnosed because the occurrence of the disease varies, depending on the severity of glucokinase impairment, from asymptomatic mild hyperglycemia over various degrees of glucose intolerance up to the development of persistent fasting hyperglycemia (15, 61). Even if some MODY 2 patients display peripheral insulin resistance, this phenomenon might be secondary to the disease rather than a direct consequence of the mutation (11). Since development of overt diabetes is quite rare in MODY 2 patients, diabetesassociated macro- and microvascular complications, overweight, and dyslipidemia are uncommon (61, 62), and patients usually manage blood glucose control by diet and exercise alone (15).

A worldwide population prevalence of 0.04–0.1% is estimated for MODY 2. The relative prevalence of the different subtypes is not exactly known, but MODY 2 is supposed to be one of the most common MODY subtypes, representing up to 63% of all MODY cases (3, 19, 62). To date, a total of 446 naturally occurring point mutations within the coding region of *GCK* have been described, but the rare incidence of MODY 2/PNDM and the genetic heterogeneity of the affected subjects impede detailed clinical studies in human medicine. For this reason, genetically modified animal models are essential to survey relevant clinical and pathophysiological aspects of this disease. However, up to now, few advances have been made in human medicine as well as in animal models to disclose the pathomorphology of this putative mild diabetes subtype (42).

The chemical mutagen N-ethyl-N-nitrosourea (ENU) has already been used in various mouse mutagenesis programs for

the production of animal models for human diseases by random mutagenesis (13). In the Munich ENU mouse mutagenesis project, mutagenized mice are examined in various phenotypic screens to characterize mouse mutants with defects of diverse organ systems or changes in metabolism (26). A screening profile of clinical chemical parameters was established to detect abnormal blood substrate and electrolyte levels or enzyme activities. Transmission of the altered phenotype to subsequent generations was confirmed by breeding of phenotypically affected mice and screening of the offspring, thereby revealing a mutation as cause for the aberrant phenotype (49, 50).

In this study, we introduce the genetic, clinical, and pathomorphological features of the Munich  $Gck^{M210R}$  mutant mouse, a new ENU-induced mouse model for MODY 2.

## RESEARCH DESIGN AND METHODS

Animals. Animals were generated in the Munich ENU mouse mutagenesis project on the genetic background of the inbred strain C3HeB/FeJ (C3H) as previously described (26, 49). Mice had free access to water and were fed ad libitum (standard rodent diet; Altromin, Lage, Germany) except for the indicated period. The numbers of animals investigated are listed in Tables 2–4 and Figs. 1–6. All animal experiments were accomplished with authorization of the responsible animal welfare authority.

Linkage analysis. For linkage analysis, male heterozygous diabetic mutant mice, on the genetic background of the inbred strain C3HeB/FeJ, were backcrossed twice to C57BL/6J female mice. From the resulting N2 progeny 75 diabetic and 15 nondiabetic mice were killed, and tissue samples for DNA isolation were collected. DNA from tail clip samples was isolated as previously described (24), and genomewide linkage analysis of the DNA samples using single nucleotide polymorphism (SNP)-based strategies was carried out subsequently by MassExtend, a matrix-assisted laser desorption ionization-time of flight (MALDI-TOF) mass spectrometry (MS) genotyping system (Sequenom, San Diego, CA).

Candidate gene analysis: sequencing of the glucokinase gene. For sequence analysis of the glucokinase gene (Gck), total RNA was isolated from liver of homozygous and heterozygous mutant animals and wild-type littermate control animals by guanidinium thiocyanatephenol-chloroform extraction. After DNase I digestion, RNA was reverse transcribed with random hexamer primers, and RT-PCR was carried out with the primer combinations illustrated in Table 1. For genomic sequence analysis of Gck, DNA was isolated from tail clips and PCR was performed with the indicated primer combinations (Table 1). PCR products were purified with the QIAquick Gel Extraction Kit (Qiagen, Hilden, Germany) and the High Pure PCR Product Purification Kit (Roche, Mannheim, Germany) and sequenced bidirectionally. The achieved sequences were aligned to the mouse Gck cDNA and genomic sequences (NCBI GenBank accession nos. NM\_010292 and NW\_001030444, respectively). The identified mutation creates a new restriction site for the enzyme BstYI. Hence, differentiation of the allelic genotype was feasible with restriction fragment length polymorphism (RFLP)-based strategies using the restriction endonuclease BstYI (New England Biolabs, Frankfurt, Germany). PCR products of mutant alleles are restricted into two fragments (200 and 143 bp), whereas wild-type PCR products show a length of 343 bp. The probability of an additional confounding ENU-induced mutation between the last two polymorphic markers with the highest linkage as well as within the region upstream of the last polymorphic marker was estimated according to the method of Keays et al. (30) (http://zeon.well.ox.ac.uk/git-bin/enuMutRat), assuming a mutation rate of 1 in 1 Mb.

Glucokinase enzyme activity. Glucokinase enzyme activity in isolated pancreatic islets and liver homogenate from 85-day-old mice was determined by an indirect fluorometric coupled assay as previ-

Table 1. Gck-specific primers for cDNA and genomic DNA sequence analysis

Oligo Name	Sequence (5'-3')	Nucleotide Position
Gck_1_for	ACACTCAGCCAGACAGTCCTC	5' UTR
Gck_2_rev	ACCACATCCATCTCAAAGTCC	599-579
Gck_3_for	ACATCGTGGGACTTCTCCGAG	539-559
Gck_4_rev	TGATGCGCATCACGTCCTCAC	1213-1193
Gck_5_rev	TGATGCGCATCACGTCCTCAC	1042-1063
Gck_6_rev	TCACTGGCTGACTTGGCTTGC	3' UTR
Gck_7_for	ATGGCTGTGGATACTACAAGG	1-21
Gck_8_rev	ATGGCATCTGGGAAACCTGAC	3' UTR
Gck_20_for	AAGAGGAAGCTGTGGCTTCAACC	5' UTR
Gck_21_rev	AGGCATAGACACTTATAGGTGGC	Intron 1
Gck_22_for	AGCCGATCCTGCTTGATTCTCC	Intron 9
Gck_24_rev	TCTCTGAATGTTTGTGGCCTG	3' UTR
Gck_25_for	ATCTCCACTACCCACAAGTCTG	5' UTR
Gck_26_rev	TCCTACAGGATCGCACTCATC	Intron 1
Lvb_Gck_1_for	CGACCGGATGGTGGATGA	819-836
Lvb_Gck_1_rev	TCATTGGCGGAAAGTACATGG	875-895

The following primer combinations were used: *I*) for cDNA sequence analysis: Gck\_1\_for and Gck\_2\_rev; Gck\_7\_for and Gck\_2\_rev; Gck\_3\_for and Gck\_4\_rev; Gck\_5\_for and Gck\_6\_rev; 2) for genomic DNA sequence analysis: Gck\_5\_for and Gck\_8\_rev; Gck\_20\_for and Gck\_21\_rev; Gck\_22\_for and Gck\_24\_rev; Gck\_25\_for and Gck\_26\_rev (pancreas-specific exon 1); *3*) for quantitative real-time PCR of *Gck*: Lvb\_Gck\_1\_for and Lvb\_Gck\_1\_rev. Nucleotide positions are according to NCBI GenBank accession nos. NM\_010292 and NW\_001030444, for cDNA and genomic sequences, respectively. UTR, untranslated region.

ously described (20, 38). Pancreatic islets were isolated by handpicking under a stereomicroscope (Zeiss, Oberkochen, Germany) after intraductal collagenase (collagenase type I, Sigma-Aldrich, St. Louis, MO) perfusion and pancreas digestion. Subsequently, islets were sonicated (Branson sonifier cell disruptor B15, Branson Ultrasonic, Danbury, CT), and the assay was conducted in the presence of 100 and 0.50 mM glucose at 30°C for 90 min. Furthermore, 20 mg of freshly isolated liver tissue was homogenized in 1 ml of buffer (20) with a Polytron PT 1200 E tissue homogenizer (Kinematica, Luzern, Switzerland) and then sonicated. Hepatic glucose phosphorylating activity was determined in the presence of either high (100, 50, 25, 12, and 6 mM) or low (0.5, 0.25, 0.125, 0.06, and 0.03 mM) glucose concentrations after incubation for 30 min at 30°C. Fluorescence was determined with a SPEKOL 1500 UV/vis spectrophotometer (Analytic Jena, Jena, Germany). Glucokinase activity was corrected for the hexokinase fraction by subtracting the activity at 0.50 mM glucose from the total activity observed in the presence of high glucose concentrations and referred to the total protein content in the homogenate, determined by the Bradford method.

Quantitative real-time PCR. Total RNA from isolated pancreatic islets was purified with the RNeasy-Mini Kit (Qiagen). Each 400 ng of total hepatic RNA isolated from liver homogenates of newborn and 85-day-old mice and each 400 ng of total islet RNA from 85-day-old mice were reverse transcribed as described above. cDNA-specific primers for amplification of mouse Gck (sequences are listed in Table 1), and the housekeeping genes  $\beta$ -actin (Actb) (41), mitochondrial ribosomal protein S9 (Mrps9) (25), and 18S ribosomal RNA (18s rRNA) (51) were chosen with Primer Express version 3.0 (Applied Biosystems) and queried by NCBI Blast software (http://blast.ncbi. nlm.nih.gov/Blast.cgi). Real-time PCR analyses were performed as previously described (25) with SensiMix Plus SYBR (Qantace, London, UK). Transcript abundances of Gck were calculated in relation to the expression of  $\beta$ -actin (41), 18S rRNA, and Mrps9 with the  $2^{-\Delta C_T}$ (where C<sub>T</sub> is threshold cycle) method (12) and showed comparable results for all three housekeeping genes.

Western blot analysis. For detection of glucokinase isoforms by Western blot analysis, isolated pancreatic islets and hepatic tissue from 85-day-old mice were subjected to protein extraction buffer [in mmol/l: 20 Tris · HCl pH 7.6, 250 NaCl, 3 EDTA, 3 EGTA, 1 phenylmethylsulfonyl fluoride (PMSF), 2 Na-orthovanadate, and 1 dithiothreitol (DTT), with 0.5% Ipegal CA 630] and sonicated. Islet and liver homogenate was centrifuged (10 min, 10,000 rpm), and protein content in the supernatant was quantified by the Bradford method. Twenty micrograms of total islet and liver protein was subjected to SDS-PAGE and transferred to a nitrocellulose membrane (Schleicher & Schüll, Dassel, Germany). The following primary antibodies were used: rabbit anti-glucokinase (1:250; Abcam, Cambridge, MA) and mouse anti-actin (1:10,000; Cell Signaling Technology, Beverly, MA). Peroxidase conjugated goat anti-rabbit IgG (Cell Signaling Technology) and rabbit anti-mouse Ig (DAKO Diagnostika, Hamburg, Germany) diluted 1:10,000 were used as secondary antibodies. Furthermore, a rabbit anti caspase-3 antibody (Cell Signaling Technology) was applied to detect the inactive and induced form of caspase-3 in pancreatic islets as an indicator of apoptosis (1:1,000). The specific bands were visualized by chemiluminescence (Luminol, Santa Cruz Biotechnology, Santa Cruz, CA) and quantified by densitometry with ImageJ software (W. S. Rasband, ImageJ, National Institutes of Health, Bethesda, MD; http://rsbweb.nih.gov/ij/).

Body weights and glucose homeostasis. The body weight of mice was first determined on the day of birth and at the age of 4 days. The body weight of ad libitum-fed 21-, 85-, and 170-day-old mice was determined to the nearest 0.1 g. The body weight of fasted mice was also quantified at the age of 30, 90, and 180 days.

Blood glucose concentrations of ad libitum-fed and fasted animals were determined at the indicated age with the GLeasy system (Dr. Müller Gerätebau, Freital, Germany).

Oral glucose tolerance tests (OGTT) were performed in 30-, 90-, and 180-day-old heterozygous mutant mice and wild-type littermate control mice as previously described (24). The homeostasis model assessment (HOMA) of  $\beta$ -cell function and the HOMA of insulin resistance (IR) indexes were calculated as follows: HOMA %B =  $20 \times \text{fasting insulin/(fasting glucose} - 3.5)$  and HOMA IR = fasting insulin  $\times$  fasting glucose/22.5 (36). Serum insulin concentrations in the fasted state and 10, 30, 60, and 120 min after oral glucose application were quantified by ELISA (Crystal Chem, Downers Grove, IL). Intraperitoneal insulin tolerance tests (ITT) were performed at 30, 85, and 170 days of age with injection of 0.75 IU of insulin (Insuman Rapid, Sanofi Aventis, Frankfurt, Germany) per kilogram of body weight intraperitoneally. Blood glucose decrease after insulin administration was measured at the indicated time points.

Pancreatic insulin content. Pancreatic insulin content of 270-dayold mice was quantified as previously described (43). Insulin content in the pancreas homogenate was determined by ELISA as described above and referred to the total protein content, quantified spectrophotometrically (Eppendorf BioPhotometer, Eppendorf, Hamburg, Germany).

Pancreas preparation and morphometric investigations. Quantitative stereological analysis of pancreas sections from neonatal and 210-day-old mice was carried out with unbiased model-independent methods (21, 64) as previously described. Briefly, the pancreas volume [V<sub>(pan)</sub>] was calculated by dividing the pancreas weight by the specific weight of mouse pancreas (1.08 mg/mm<sup>3</sup>). The volume density of islets in the pancreas [Vv(islets/pan)] was calculated by dividing the sum of cross-sectional areas  $(\sum A)$  of islet profiles by the  $\sum A$  of the pancreas. The total islet volume [ $V_{(islets,pan)}$ ] was calculated by multiplying  $Vv_{(islets/pan)}$  and  $V_{(Pan)}$ . The volume density of  $\beta$ -cells in the islets  $[Vv_{(\beta\text{-cells/islets})}]$  was obtained by dividing  $\sum A$   $\beta$ -cells and  $\sum A$  islets; the total  $\beta$ -cell volume  $[V_{(\beta\text{-cells,pan})}]$  was attained by multiplying  $V_{(\beta\text{-cells/islets})}$  and  $V_{(islets,pan)}$  (23–24). Additionally, the volume density of the  $\beta$ -cells  $[Vv_{(\beta-cells/pan)}]$  in the pancreas of newborn male mice was calculated by dividing the sum of crosssectional areas of  $\beta$ -cells by  $\Sigma A$  of the pancreas.  $V_{(\beta\text{-cells,pan})}$  was determined by multiplying  $Vv_{(\beta\text{-cells/pan})}$  and  $V_{(pan)}$ .

Immunohistochemistry. Insulin-containing  $\beta$ -cells in pancreas sections were detected by the indirect immunoperoxidase method as previously described (23). Horseradish-conjugated rabbit anti-guinea pig IgG was obtained from DAKO Diagnostika.  $\beta$ -Cell apoptosis in pancreas sections was determined by TdT-mediated dUTP-biotin nick end labeling (TUNEL) (ApopTag Peroxidase In Situ Apoptosis Detection Kit, Millipore) and coimmunohistochemical staining for insulin.

Data presentation and statistical analysis. All data are means  $\pm$  SD. Statistical analyses were performed with Student's *t*-test. *P* values <0.05 were considered significant.

#### RESULTS

Establishment of the diabetic mouse strain. In the clinical chemical screen (49) for dominant mutations, accomplished in the context of the Munich ENU mouse mutagenesis project (26), a male F1 offspring of an ENU-treated C3H mouse was identified exhibiting elevated fasting plasma glucose concentrations (>235 mg/dl). Inheritance of the abnormal phenotype was tested as previously described (2). After confirmation of an autosomal dominant inheritance of the diabetic phenotype, male hyperglycemic mice were mated to wild-type C3H females to establish the mutant strain GLS001.

Linkage analysis, candidate gene sequencing, and genotyping. The SNP analysis, using a genome-wide mapping panel comprising a total number of 136 polymorphic markers, revealed a strong linkage ( $\chi^2 = 64.66$ ; P < 0.0001) of the diabetic phenotype to the marker rs13480881, localized at the proximal region of chromosome 11. Sequencing of the positional candidate gene Gck disclosed a T  $\rightarrow$  G transversion at nucleotide position 629 in exon 6 of Gck (NCBI GenBank accession no. NM 010292) (Fig. 1, A and B). The probability of an additional confounding ENU-induced mutation between the two polymorphic markers with the highest linkage as well as within the region upstream of the polymorphic marker with the highest linkage was 0.0006 and 0.0045, respectively (http:// zeon.well.ox.ac.uk/git-bin/enuMutRat). The mutation leads to an amino acid exchange from methionine to arginine at position 210. According to the mutation, the official term Munich GckM210R mutant mouse was chosen for this hyperglycemic strain. The single base pair substitution from T to G creates a new restriction site for the enzyme BstYI. Hence, differentiation of the allelic genotype was feasible with RFLP-based strategies (Fig. 1*C*).

Glucokinase enzyme activity. The fluorometric coupled assay carried out with liver homogenate showed a significantly reduced hepatic glucokinase phosphorylating activity in heterozygous Munich  $Gck^{M210R}$  mutant mice (by  $\sim 50\%$  vs. wildtype mice) (Fig. 1, D and E), whereas islet glucokinase activity and hepatic and islet hexokinase activities were not significantly altered. Nevertheless, in pancreatic islets, hexokinase activity was about sixfold higher than glucokinase activity, whereas in liver hexokinase activity contributed only to a minor extent to the total hepatic phosphorylating activity (Fig. 1, E and E).

Quantitative real-time PCR. The relative Gck transcript abundance in liver homogenates from newborn mice was significantly reduced in both homozygous and heterozygous mutant mice versus wild-type mice and in homozygous versus heterozygous mutant mice (Fig. 1G). In contrast, at the age of 85 days, relative Gck transcript abundance of heterozygous

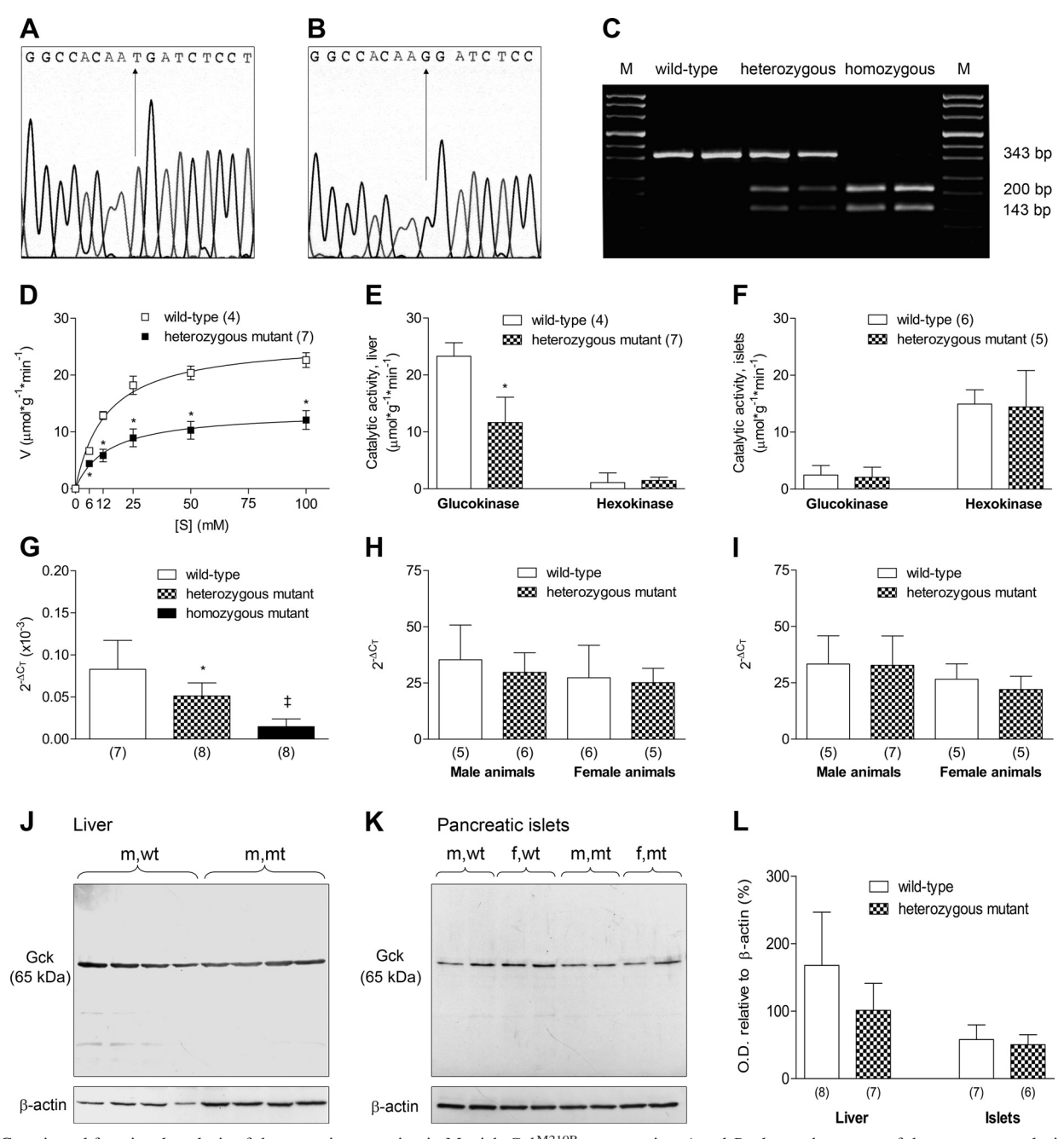


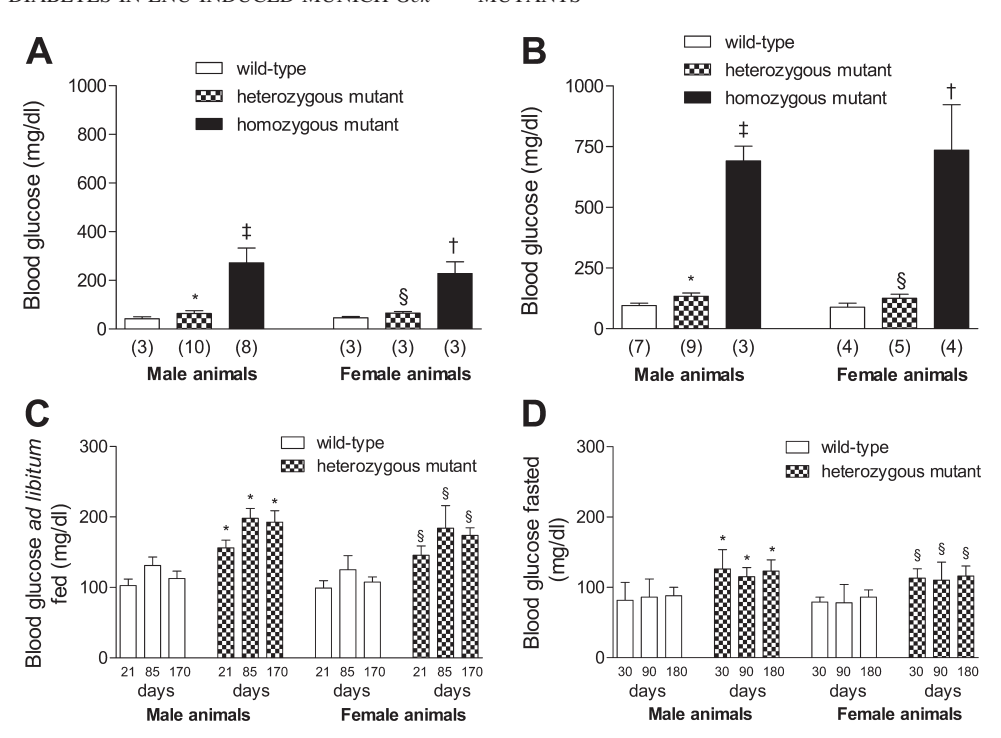
Fig. 1. Genetic and functional analysis of the causative mutation in Munich  $Gck^{M210R}$  mutant mice. A and B: electropherogram of the sequence analysis of Gck in wild-type control (A) and homozygous mutant (B) mice. The position of the base exchange at nucleotide 629 is marked by an arrow. C: genotype-specific restriction fragment length polymorphism (RFLP) analysis showed no restriction site in the wild-type allele (343 bp) and 2 fragments (200 bp, 143 bp) for the mutant allele, B0, fragment size marker. B1: glucokinase enzyme activity (reaction velocity, B1) in liver homogenate extracted from 85-day-old animals, in presence of 100, 50, 25, 12, and 6 mM glucose [S]. B2 and B3: hepatic (B3) and islet (B4) and islet (B4) moreover a service from 85-day-old mice relative to B5. B6, actin) transcript abundances in liver homogenates from newborn mice (B5) and in liver (B6) and islet (B7) homogenates from 85-day-old mice relative to B7. The shold cycle. B8-class activity in PcR2 and isolated pancreatic islets from 85-day-old mice (B8) and quantitative analysis of the relative optical density (OD) (B8). Data represent means and SD; nos. of mice examined per group are presented in parentheses; B8 and quantitative analysis of the relative optical density (OD) (B8). Data represent means and SD; nos. of mice examined per group are presented in parentheses; B8 and quantitative analysis of the relative optical density (OD) (B8). Data represent means and SD; nos. of mice examined per group are presented in parentheses; B8 and quantitative analysis of the relative optical density (OD), and present means and SD; nos. of mice examined per group are presented in parentheses; B8 and B9 are controlled by an arrow B9 and B9 and B9 are controlled by an arrow B9 and B9 are controlled by an arrow B9 and B9 are controlled by an arrow B

mutants was unchanged in liver homogenate (Fig. 1H) and in pancreatic islets (Fig. 1I) compared with wild-type mice.

Western blot analysis. Glucokinase protein levels of 85-dayold heterozygous mutants were decreased by tendency in liver homogenate (Fig. 1, J and L) but unchanged in pancreatic islets (Fig. 1, K and L) compared with wild-type control mice. Furthermore, no induction of caspase-3 as an indicator of apoptosis was detectable in heterozygous mutant animals of either sex (see Fig. 5*F*).

Glucose homeostasis of heterozygous Munich Gck<sup>M210R</sup> mutant mice. Heterozygous mutant mice showed slightly but significantly elevated ad libitum-fed blood glucose levels from

Fig. 2. Ad libitum-fed and fasting blood glucose concentrations in heterozygous and homozygous mutant mice. A-C: ad libitumfed blood glucose at birth (A), at 4 days of age (B), and at 21, 85, and 170 days of age (C). D: fasting blood glucose levels at 30, 90, and 180 days of age. All data represent means and SD; nos. of mice examined per group are in parentheses. C and D: investigations were carried out with 10 animals per group. \*P < 0.05, male heterozygous mt vs. male wt;  $\S P < 0.05$ , female heterozygous mt vs. female wt;  $\ddagger P < 0.05$  male homozygous mt vs. male wt and male heterozygous mt;  $\dagger P < 0.05$  female homozygous mt vs. female wt and female heterozygous mt.



the first days of life onward (Fig. 2, A and B). Disturbance in glucose homeostasis of these mutants deteriorated little until 85 days of age, remaining stable thenceforth (Fig. 2C). At 30 days of age, fasting blood glucose levels were found to be significantly elevated in both heterozygous male and female mutant animals and remained stable during the period investigated (Fig. 2D).

During OGTT, 30-day-old male and female heterozygous mutant animals showed significantly elevated blood glucose levels until 90 min after oral glucose application. At 120 min, blood glucose concentrations of heterozygous mutant mice were similar to those of wild-type mice (Fig. 3A). At the ages of 90 and 180 days, blood glucose concentrations of heterozygous mutant animals were significantly increased at all time points during OGTT compared with age- and sex-matched wild-type animals (Fig. 3B; Table 2). The area under the glucose curve (AUC) was already significantly increased in 30-day-old heterozygous mutant mice of both sexes and further deteriorated with age, while the AUC of wild-type mice remained almost constant until an age of 180 days (Fig. 3C).

Fasting serum insulin levels were significantly decreased in 90- and 180-day-old male heterozygous mutant mice, and both sexes of all examined age groups displayed significantly reduced insulin secretion after oral glucose administration (Fig. 3, D and E). During OGTT performed with 90-day-old mice, serum insulin levels were significantly reduced until 30 min after oral glucose application in male and until 10 min in female mutant mice. Furthermore, male heterozygous mutant mice exhibited a significantly decreased AUC insulin during OGTT at an age of 90 days, whereas the AUC insulin was only slightly reduced in female mutant mice (Fig. 3F). Consequently, the HOMA of  $\beta$ -cell function index was reduced by  $\sim$ 75% in male and female heterozygous mutant mice compared with sex-matched control mice (Fig. 3G).

At an age of 30 days, blood glucose decrease during ITT was comparable between heterozygous mutant and wild-type mice (Table 3), while 85- and 170-day-old male mutant mice showed a significantly less pronounced decrease of blood glucose levels from basal 10 min after intraperitoneal insulin application versus male control mice (Fig. 3*H*; Table 3). However, the HOMA IR index of male mutant mice was not altered (Fig. 3*I*).

Clinically relevant parameters in homozygous mutant mice. Homozygous mutant mice were born as expected according to the Mendelian pattern of inheritance. Already at the first day postpartum, homozygous mutant mice showed marked glucosuria and dramatically elevated blood glucose concentrations with severe deterioration of the diabetic phenotype until the age of 4 days (Fig. 2, A and B). The birth weight of homozygous mutant mice was not different compared with heterozygous mutant and wild-type control mice (Fig. 4A) but did not increase during the first days of life. At the age of 4 days, the body weight of homozygous mutant mice was <50% that of age-matched control mice (Fig. 4B). Homozygous mutant mice died of severe diabetes mellitus not later than 6 days postpartum. The mean survival period of homozygous mutant mice was ~4 days, whereas life expectancy of heterozygous mutant in relation to wild-type animals was not constrained (Fig. 4, C and D).

Qualitative histological and quantitative stereological investigations of pancreas and pancreatic insulin content. Macroscopically and histologically, pancreata from newborn heterozygous and homozygous mutant mice as well as from 210-day-old heterozygous mutant mice appeared normal, and no evidence for any inflammatory event in the islets was detectable. Insulin immunostaining of pancreas sections from these mutant mice revealed typical islet composition and distribution of insulin-positive cells within the islets.  $\beta$ -Cell staining intensity for insulin was also comparable to that in control mice (Fig. 5, A–E).  $V_{(pan)}$  (Fig. 6A),  $V_{V_{(\beta-cells/pan)}}$  (Fig. 6B), and  $V_{(\beta-cells,pan)}$  (Fig. 6C) of neonatal heterozygous and homozygous male mutant mice were unchanged versus wild-type

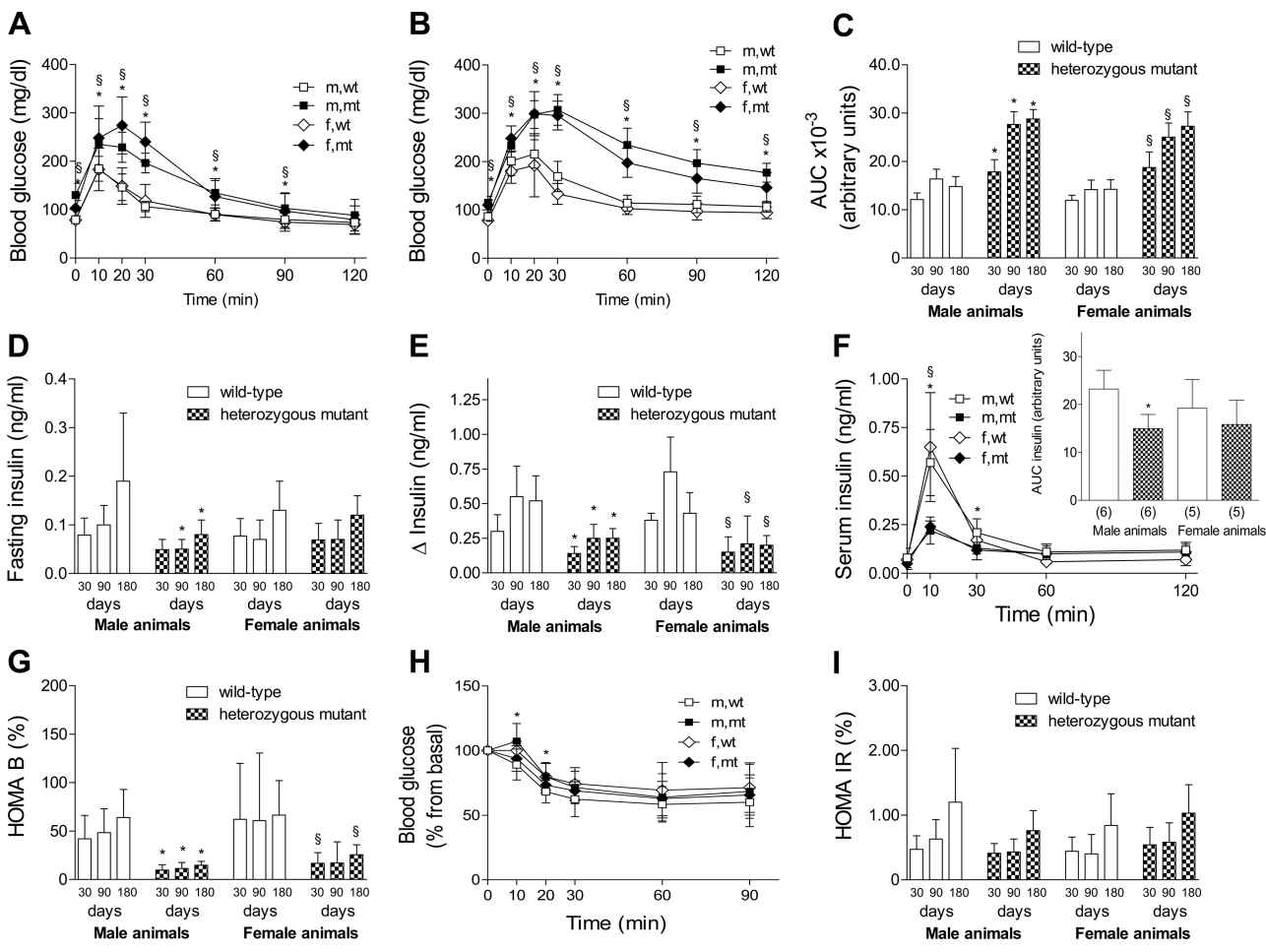


Fig. 3. Functional glucose and insulin tests in heterozygous mutant mice. A and B: oral glucose tolerance test of 30 (A)- and 90 (B)-day-old mice. C: area under the glucose curve (AUC) during oral glucose tolerance test. D: fasting serum insulin levels. E: glucose-induced insulin secretion ( $\Delta$  insulin). F: serum insulin concentrations and area under the insulin curve (AUC, *inset*) during oral glucose tolerance test in 90-day-old mice. G: homeostasis model assessment of baseline insulin secretion (HOMA B). H: intraperitoneal insulin tolerance test of 170-day-old mice. I: homeostasis model assessment of insulin resistance (HOMA IR). Data represent means and SD. In F, *inset*, nos. of animals examined per group are presented in parentheses; other tests were carried out with 10 animals per genotype and sex. \*P < 0.05, male heterozygous mt vs. male wt; P < 0.05, female heterozygous mt vs. female wt.

mice. Likewise,  $V_{(pan)}$  (Table 4) and  $Vv_{(\beta\text{-cells/islets})}$  (Fig. 6*E*) were not altered in 210-day-old mutant versus control mice.  $Vv_{(islets/pan)}$ ,  $V_{(islets,pan)}$ , and the total  $\beta$ -cell volume  $[V_{(\beta\text{-cells,islets})}]$  of heterozygous male, but not female mutant mice was significantly decreased versus age- and sex-matched control mice (Fig. 6, *D*, *G*, and *H*). Additionally, the volume density of isolated  $\beta$ -cells in the pancreas  $[Vv_{(isolated \beta\text{-cells/pan})}]$  and the total volume of isolated  $\beta$ -cells  $[V_{(isolated \beta\text{-cells,pan})}]$  were significantly de-

Table 2. Blood glucose concentrations during oral glucose tolerance test in heterozygous mutant versus wild-type control mice at age of 180 days

		Time After Glucose Challenge, min					
	0	10	20	30	60	90	120
m, wt	86 (12)	180 (38)	154 (34)	149 (29)	112 (14)	105 (13)	103 (18)
m, mt	<b>123</b> (16)	<b>245</b> (33)	<b>282</b> (28)	<b>302</b> (22)	<b>242</b> (25)	<b>217</b> (19)	204 (22)
f, wt	86 (10)	172 (31)	159 (34)	123 (18)	105 (12)	116 (44)	93 (15)
f, mt	<b>114</b> (15)	<b>251</b> (32)	<b>302</b> (57)	<b>266</b> (46)	<b>216</b> (45)	<b>191</b> (38)	<b>174</b> (36)

Data are means (SD); n = 10/group; m, male; f, female; mt, heterozygous mutant mice; wt, wild-type mice. Bold numbers, P < 0.05.

creased in 210-day-old male heterozygous mutant mice (Fig. 6, F and I). Combined TUNEL-insulin immunostaining of pancreas sections of 210-day-old male mice could not demonstrate any apoptotic  $\beta$ -cells in the investigated islets of wild-type and heterozygous mutant mice, whereas occasional apoptotic cells were observed in the exocrine pancreas and lymph nodes. The pancreatic insulin content of 270-day-old male heterozygous mutant mice was only marginally reduced compared with wild-type mice (Fig. 5H).

# DISCUSSION

In this study, the genetic, clinical, and pathomorphological features of the Munich  $Gck^{\rm M210R}$  mutant mouse as a new mouse model for MODY 2 were specified.

Breeding heterozygous mutants to C3H wild-type mice over >10 generations led to the loss of noncausative, clinically unapparent ENU-induced mutations. The occurrence of the diabetic phenotype remained unaltered in ensuing generations, giving proof of the heritability and the complete penetrance of the abnormal phenotype. Together with the results of the linkage analysis these findings indicate that the identified

Table 3. Change of blood glucose levels during insulin tolerance tests of 30- and 85-day-old heterozygous mutant versus wild-type control mice

		Time After Insulin Application, min			
	10	20	30	60	90
		30-day-	old mice		
m, wt	106 (15)	84 (11)	79 (9)	61 (18)	65 (19)
m, mt	119 (11)	90 (12)	79 (9)	68 (11)	69 (20)
f, wt	114 (18)	87 (5)	83 (8)	60 (19)	59 (17)
f, mt	116 (14)	82 (6)	77 (6)	61 (10)	68 (11)
		85-day-	old mice		
m, wt	99 (8)	74 (8)	66 (9)	62 (13)	72 (15)
m, mt	107 (8)	80 (14)	70 (10)	71 (13)	87 (14)
f, wt	97 (14)	74 (17)	69 (19)	56 (21)	57 (19)
f, mt	102 (13)	75 (8)	63 (5)	51 (11)	47 (14)

Data represent means (SD); n=5 (30 days old) and 10 (85 days old) per group. Change of blood glucose is illustrated as % from basal levels. Bold numbers, P<0.05.

missense mutation in the glucokinase gene is causative for the diabetic phenotype of the mouse strain.

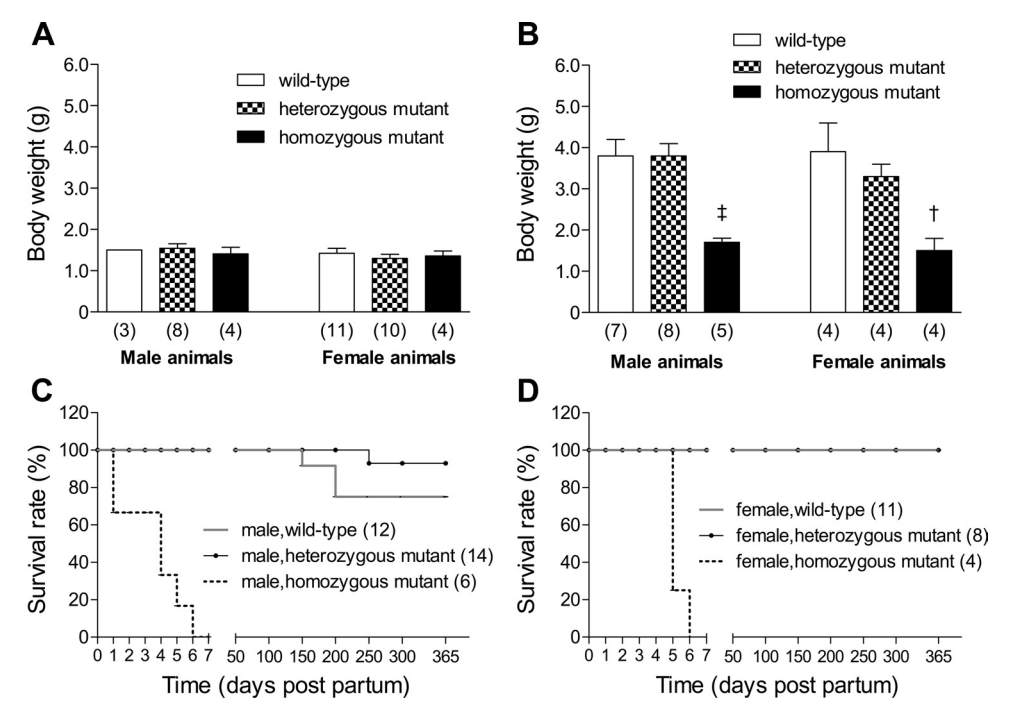
The catalytic enzyme glucokinase is known to play a central role in glucose homeostasis. In hepatocytes glucokinase facilitates glucose uptake and controls glycogen synthesis (46), whereas in pancreatic  $\beta$ -cells it catalyzes the first, rate-limiting step of glycolysis and is therefore considered a glucose sensor (19, 35). Hence, already minimal changes in glucokinase enzyme activity can entail serious consequences for the organism, because the threshold for glucose-induced insulin secretion is directly altered (46).

Various *Gck*-deficient mouse models have already been generated (6, 20, 46, 47, 55). Rodent models that exhibit point mutations in *Gck* resemble the situation in human MODY 2/PNDM and provide the opportunity for the functional analysis of *Gck*. Fifteen diabetic mouse strains with inactivating

mutations in Gck, showing phenotypes similar to MODY 2 in human patients, have been identified in various ENU mutagenesis projects so far (17, 27, 57) (http://www.brc.riken.jp/lab/gsc/mouse), but detailed pathomorphological characterization of these strains is lacking. In addition, the Munich  $Gck^{M210R}$  mutant mouse is the first strain that exhibits a mutation at amino acid position M210. Four inactivating M210 mutations have already been reported in human diabetic patients (42, 52, 60). Therefore, Munich  $Gck^{M210R}$  mutant mice represent a valuable model to gain more insights into relevant clinical and pathomorphological aspects of the human disease.

For the majority of ENU-induced Gck mutant strains, the mutation was found to result in significantly reduced glucokinase activity (27, 57), and the human M210K mutation was also shown to be associated with reduced enzyme activity in vitro (39). Likewise, hepatic glucokinase activity was decreased in heterozygous Munich GckM210R mutant mice, demonstrating that the identified mutation is causative for the diabetic phenotype. The fact that islet glucokinase activity in heterozygous mutant mice was obviously unaffected might be caused by the predominance of low-affinity hexokinase activity in pancreatic islets, which probably impedes the identification of potential differences of islet glucokinase activity (58). Additionally, the mutation leads to a significant reduction of hepatic Gck expression in newborn homozygous and heterozygous Munich  $Gck^{M210R}$  mutant mice. In adult heterozygous mutant mice, hepatic Gck and islet Gck mRNA levels were unaltered, most likely as a consequence of efficient compensatory mechanisms, such as overexpression of the wild-type allele (59). The initial decrease of hepatic Gck transcript abundance in neonatal mutant mice might reflect the lack of compensatory overexpression of the wild-type allele at this age. Consistent with these findings, hepatic glucokinase protein levels were only slightly reduced and islet glucokinase protein abundance was unaltered in heterozygous mutant mice compared with wild-type littermates. The mutation M210K has already been

Fig. 4. Body weight and life expectancy in heterozygous and homozygous mutant mice. A: birth weight. B: body weight at 4 days of age. C and D: life expectancy of heterozygous and homozygous male (C) and female (D) mutant mice vs. wild-type control mice. Data represent means and SD.  $\ddagger P < 0.05$ , male homozygous mt vs. male wt and male heterozygous mt vs. female wt and female heterozygous mt. Nos. of animals examined per group are presented in parentheses.



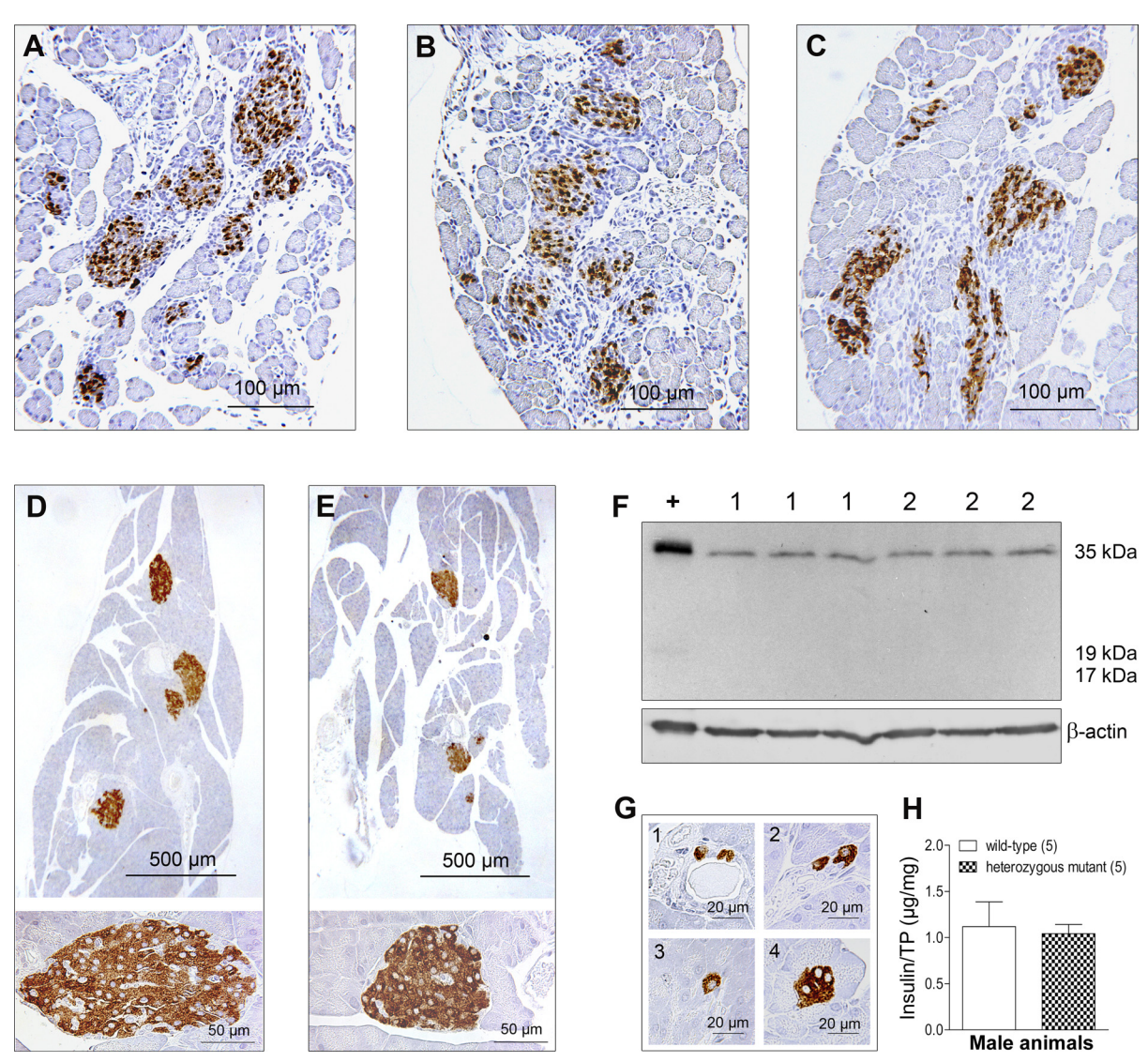


Fig. 5. A–E: insulin immunohistochemistry of pancreas sections at the 1st day postpartum (A–C) and at an age of 210 days (D, E). F: caspase-3 Western blot from pancreatic islet isolates (85 days of age). G and H: exemplary illustration of isolated G-cells (G) and pancreatic insulin content (H). In neonatal mice, staining intensity of the insulin-producing G-cells and the cross-sectional area of G-cells in the pancreas do not differ in male homozygous (G) and heterozygous (G) animals. At 210 days of age, staining intensity and distribution of the insulin-producing G-cells in the islets do not differ between male heterozygous mutants (G, G) and male wild-type control (G), G0, G1 animals, whereas islets are conspicuously smaller in heterozygous mutant (G2, G3) bottom) wild-type (G3), G4 bottom) mice. G5: immunoblotting of pancreatic islet isolates from 85-day-old mice revealed no induction of caspase-3 in male wild-type mice (G3) and male heterozygous mutant mice (G3), whereas the 19-kDa fragment of the cleaved caspase-3 (active) was detectable in the positive control (G4), G5: spectrum of insulin-G6: spectrum of insulin-G7 stained pancreatic cells, classified as isolated G6-cells: insulin-positive cells within (G3) or budding from pancreatic ducts (G3), and extra-islet G6-cell clusters (G6-cells) (G8. G9-cells) (G9-cells) (G9-cel

shown to be refractory to glucokinase activators as well as to increasing concentrations of glucokinase regulatory protein (GKRP), which is known to be critically involved in posttranscriptional and posttranslational regulation of hepatic glucokinase. Therefore, impaired interaction with GKRP might account for the marginal reduction of hepatic glucokinase protein abundance in Munich  $Gck^{M210R}$  mutant mice (8, 16, 52). Reductions of Gck expression and glucokinase protein levels have also been reported to be a consequence of glucokinase mutations in ENU-induced mutants (27, 57).

Since in heterozygous mutant mice glucokinase activity was reduced to 50% of the wild-type catalytic enzyme activity, they exhibited slightly elevated blood glucose levels already from

birth, with development of glucose intolerance and stable fasting hyperglycemia from 30 days of age. In contrast, homozygous mutant mice showed severe hyperglycemia at the first day of life, with a dramatic increase of blood glucose levels within 1 day, suggesting that glucokinase activity is drastically reduced in these animals. The exacerbated phenotype of homozygous mutants resembles that of PNDM in humans, where a homozygous M210 mutation has also been identified (39, 40).

Similar to clinical findings in MODY 2 patients (22), hyperglycemia in heterozygous mutant mice was chronic but mild with slight deterioration of blood glucose concentrations until the age of 85 days, followed by stabilization of the diabetic

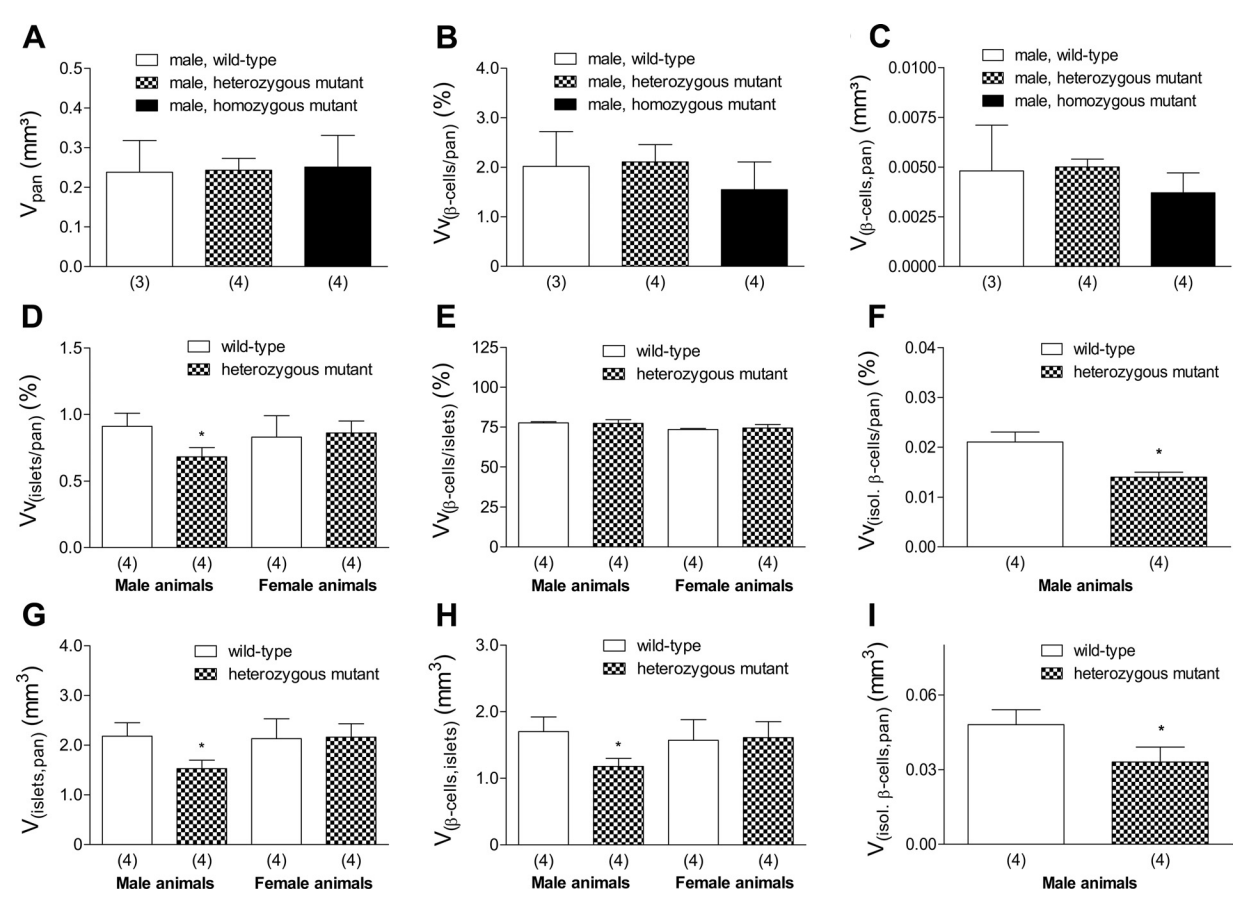


Fig. 6. Quantitative stereological analysis of the pancreas at the 1st day postpartum (A–C) and at the age of 210 days (D–I). Pancreas volume [ $V_{(pan)}$ , A], volume density of  $\beta$ -cells in the pancreas [ $V_{V(\beta\text{-cells/pan)}}$ , B], and total  $\beta$ -cell volume [ $V_{(\beta\text{-cells,pan)}}$ , C] are unaltered in both neonatal homozygous and heterozygous male mutant vs. control mice. At the age of 210 days, volume densities of islets in the pancreas [ $V_{V(\text{islets/pan)}}$ , D] and isolated  $\beta$ -cells in the pancreas [ $V_{V(\text{islets/pan)}}$ , F] are significantly reduced in male heterozygous mutant vs. control mice, whereas volume density of the  $\beta$ -cells in the islets [ $V_{V(\beta\text{-cells/islets})}$ , E] is unchanged in these animals. Consequently, total volume of islets [ $V_{(\text{islets,pan)}}$ , F], the total  $\beta$ -cell volume [ $V_{(\beta\text{-cells,islets})}$ , H], and the total volume of isolated  $\beta$ -cells [ $V_{(\text{isol}})$ ,  $V_{(\text{isol})}$ ,  $V_{$ 

phenotype. Because of this lenient and stable phenotype, life expectancy was not reduced in heterozygous mutant mice, whereas the mutation is lethal soon after birth when present on both alleles. A comparable limitation of life expectancy was observed in other homozygous murine glucokinase mutants (27) as well as in homozygous global and  $\beta$ -cell-specific Gck knockout mice (6, 20, 46, 47, 55). Because glucokinase represents the limiting factor for glucose-induced insulin release, insulin secretion after glucose application was considerably reduced in heterozygous mutant mice. Additionally, male mutant mice showed significantly reduced fasting serum insulin concentrations, a significantly reduced insulin secretory capacity, and a decelerated response to exogenous insulin, even if the

Table 4. Pancreas volume of 210-day-old heterozygous mutant versus wild-type mice

	Pancreas Volume, mm <sup>3</sup>
m, wt	239.38 (12.34)
m, mt	224.98 (3.19)
f, wt	257.13 (18.02)
f, mt	250.35 (23.06)

Data are means (SD); n = 4 per group.

HOMA IR was not altered. Despite frequent use of HOMA indexes in animal models, HOMA indexes have not been validated for use in animals (63). Therefore, the reproducible results from ITT seem to more reliably reflect insulin sensitivity in Munich  $Gck^{M210R}$  mutant mice. A slight reduction of insulin sensitivity has already been reported in other ENU-induced Gck mutant mice and can also occur in human MODY 2 patients, whereas decreased fasting insulin levels have not been detected in other Gck mutant or knockout mice so far and fasting insulin levels are usually normal in human MODY 2 patients (22, 27, 47). The slightly milder phenotype observed in female mutants is a phenomenon that has been described for several diabetic rodent models (33) and also appears in human diabetes mellitus (18). A positive impact of 17β-estradiol has been postulated to account for this sexual dimorphism (32, 33).

Pancreas weight, gross morphology, and histological appearance of the exocrine pancreas of newborn heterozygous and homozygous mutant and 210-day-old heterozygous mutant mice were unaltered. Quantitative stereological investigations of pancreatic tissue from neonatal animals revealed a comparable volume density of  $\beta$ -cells in the pancreas and an unaltered total  $\beta$ -cell volume in heterozygous and homozygous male mutant versus wild-type control mice. In contrast, a 30%

reduction of islet and β-cell mass was identified in 210-day-old male heterozygous Munich Gck<sup>M210R</sup> mutant mice, whereas both parameters were unchanged in female mutant mice, whose  $\beta$ -cells are probably protected by 17 $\beta$ -estradiol (32). Despite reduced total islet and total β-cell volumes, pancreatic insulin content was not reduced in male heterozygous mutant mice. Because blood glucose levels are known to positively regulate insulin synthesis on transcriptional and posttranscriptional levels, mild hyperglycemia of mutants might mediate insulin accumulation in β-cells of male heterozygous Munich Gck<sup>M210R</sup> mutant mice (4). Furthermore, recent studies showed that alteration of Gck expression does not lead to alterations of islet insulin content (7, 54). Since endocrine cells budding from ducts and single extra-islet insulin<sup>+</sup> cell clusters (EICs) are considered a parameter for new islet formation (23, 29), a coincident reduction of the total volume of isolated  $\beta$ -cells of male heterozygous mutant mice of ~30% and the absence of apoptosis in pancreatic islets isolated from 85-day-old mice suggests that reduced islet and β-cell mass, observed in male mutant mice, emerge from impaired islet neogenesis.

Morphological alterations of the endocrine pancreas are reported to arise in some MODY subtypes (28). Even though actual interest in the role of glucokinase in regulation of  $\beta$ -cell mass has risen, only few perceptions about the pathomorphology of MODY 2 and the influence of glucokinase aberrations on maintenance, adaptation, and turnover of the endocrine pancreatic mass are existing (42).

Over the last decades there has been increasing evidence that, from embryogenesis to adulthood, the endocrine pancreas represents a dynamic, in adult life slowly renewing, tissue whose mass is determined by the balance between replication, neogenesis, and apoptosis—under physiological conditions and in response to varying secretory demand (1, 37). The factors involved in regulating  $\beta$ -cell mass are numerous (1), but the potent stimulatory effect of glucose and insulin on the expansion of  $\beta$ -cell mass in vivo (9, 44) and in vitro (48, 53) substantiates a central impact of glucose metabolism and insulin signaling pathway on endocrine pancreatic mass expansion. Islet neogenesis and  $\beta$ -cell proliferation from preexisting β-cells are reported to be the main mechanisms of these adaptive changes (1, 10, 45). For one of these mechanisms, glucokinase has already been shown to be essential: mice haploinsufficient for pancreatic Gck failed to increase β-cell mass in response to a high-fat diet, whereas wild-type control mice developed compensatory  $\beta$ -cell hyperplasia. However, in contrast to Munich  $Gck^{M210R}$  mutant mice, no reduction of  $\beta$ -cell mass or islet size was detected in  $\beta$ -cell-specific heterozygous Gck knockout mice versus wild-type mice when fed a standard chow (56). Because the genetic background has a great influence on the occurrence of an aberrant phenotype (5), these different observations might be explained by the different genetic background of the Gck mutant mice. Additionally, parameters of islet neogenesis and the influence of the complete absence of  $\beta$ -cell glucokinase on the integrity of the endocrine pancreas were not investigated in these knockout models.

Although recent studies suggest a contrary detrimental influence of glucokinase on endocrine pancreatic mass dynamics by demonstrating that glucokinase is involved in glucotoxicity-induced β-cell death via induction of Bad dephosphorylation and Bax- and Bad-mediated apoptosis (14, 31), our data indi-

cate that impaired islet neogenesis rather than enhanced apoptosis is causative for islet and  $\beta$ -cell mass reduction in male heterozygous Munich  $Gck^{M210R}$  mutant mice.

In light of these findings, glucokinase may have an important impact on the balance between  $\beta$ -cell renewal and death and, therefore, on endocrine pancreas plasticity.

In summary, we identified a new ENU-induced Gck mutation in mice, with relevance in humans, leading to MODY 2 or PNDM. Furthermore, we showed that this Gck mutation leads to pancreatic islet and  $\beta$ -cell mass reduction in male heterozygous mutant mice, most likely as a consequence of decreased postnatal islet neogenesis. This profoundly characterized new MODY 2 model is thought to be valuable to study the roles of Gck, disturbed glucose homeostasis, and mild hyperglycemia in endocrine pancreatic mass dynamics, for the development of strategies for early diagnosis, and for the development of potential novel therapeutics.

# ACKNOWLEDGMENTS

We thank the Helmholtz Zentrum Munich for generously providing stock mice, especially Corinna Moerth for technical assistance. Furthermore, we show our gratitude to Marion Schuster and Lisa Pichl for their dedicated technical assistance and to Sabine Zwirz and Adrian Ciolovan for excellent animal management.

#### **GRANTS**

This study was supported by the Deutsche Forschungsgemeinschaft (GRK 1029; L. van Bürck, N. Herbach, B. Aigner, R. Wanke), the German Human Genome Project (DHGP), and the National Genome Research Network (NGFN; to M. Hrabé de Angelis, E. Wolf)

### DISCLOSURES

The authors are not aware of financial conflict(s) with the subject matter or materials discussed in this manuscript with any of the authors, or any of the authors' academic institutions or employers.

## REFERENCES

- 1. **Ackermann AM, Gannon M.** Molecular regulation of pancreatic betacell mass development, maintenance, and expansion. *J Mol Endocrinol* 38:
- Aigner B, Rathkolb B, Herbach N, Hrabé de Angelis M, Wanke R, Wolf E. Diabetes models by screen for hyperglycemia in phenotypedriven ENU mouse mutagenesis projects. Am J Physiol Endocrinol Metab 294: E232–E240, 2008.
- American Diabetes Association. Diagnosis and classification of diabetes mellitus. Diabetes Care 32: S62–S67, 2009.
- Andrali SS, Sampley ML, Vanderford NL, Ozcan S. Glucose regulation of insulin gene expression in pancreatic beta-cells. *Biochem J* 415: 1–10, 2008
- Andrikopoulos S, Massa CM, Aston-Mourney K, Funkat A, Fam BC, Hull RL, Kahn SE, Proietto J. Differential effect of inbred mouse strain (C57BL/6, DBA/2, 129T2) on insulin secretory function in response to a high fat diet. J Endocrinol 187: 45–53, 2005.
- Bali D, Svetlanov A, Lee HW, Fusco-DeMane D, Leiser M, Li B, Barzilai N, Surana M, Hou H, Fleischer N, DePinho R, Rossetti L, Efrat S. Animal model for maturity-onset diabetes of the young generated by disruption of the mouse glucokinase gene. *J Biol Chem* 270: 21464– 21467, 1995.
- Baltrusch S, Langer S, Massa L, Tiedge M, Lenzen S. Improved metabolic stimulus for glucose-induced insulin secretion through GK and PFK-2/FBPase-2 coexpression in insulin-producing RINm5F cells. *Endocrinology* 147: 5768–5776, 2006.
- Baltrusch S, Tiedge M. Glucokinase regulatory network in pancreatic β-cells and liver. *Diabetes* 55: S55–S64, 2006.
- Bernard C, Berthault MF, Saulnier C, Ktorza A. Neogenesis vs. apoptosis as main components of pancreatic beta cell mass changes in glucose-infused normal and mildly diabetic adult rats. FASEB J 13: 1195–1205, 1999.

- Bouwens L, Kloppel G. Islet cell neogenesis in the pancreas. Virchows Arch 427: 553–560, 1996.
- Clement K, Pueyo ME, Vaxillaire M, Rakotoambinina B, Thuillier F, Passa P, Froguel P, Robert JJ, Velho G. Assessment of insulin sensitivity in glucokinase-deficient subjects. *Diabetologia* 39: 82–90, 1996.
- Cohen CD, Kretzler M. Gene expression analysis of microdissected renal biopsies. In: *Renal Disease: Techniques and Protocols*, edited by Goligorsky M. Totowa, NJ: Humana, 2003, p. 285–293.
- 13. **Cordes SP.** *N*-ethyl-*N*-nitrosourea mutagenesis: boarding the mouse mutant express. *Microbiol Mol Biol Rev* 69: 426–439, 2005.
- 14. Danial NN, Gramm CF, Scorrano L, Zhang CY, Krauss S, Ranger AM, Datta SR, Greenberg ME, Licklider LJ, Lowell BB, Gygi SP, Korsmeyer SJ. BAD and glucokinase reside in a mitochondrial complex that integrates glycolysis and apoptosis. *Nature* 424: 952–956, 2003.
- Fajans SS, Bell GI, Polonsky KS. Molecular mechanisms and clinical pathophysiology of maturity-onset diabetes of the young. N Engl J Med 345: 971–980, 2001.
- Farrelly D, Brown KS, Tieman A, Ren J, Lira SA, Hagan D, Gregg R, Mookhtiar KA, Hariharan N. Mice mutant for glucokinase regulatory protein exhibit decreased liver glucokinase: a sequestration mechanism in metabolic regulation. *Proc Natl Acad Sci USA* 96: 14511–14516, 1999.
- Fenner D, Odili S, Takahashi JS, Matschinsky FM, Bass J. Insight into glucokinase diabetes from ENU mutagenesis (Abstract). *Diabetes* 58, Suppl 1: A308, 2009.
- Gale EA, Gillespie KM. Diabetes and gender. Diabetologia 44: 3–15, 2001
- Gloyn AL. Glucokinase (GCK) mutations in hyper- and hypoglycemia: maturity-onset diabetes of the young, permanent neonatal diabetes, and hyperinsulinemia of infancy. *Hum Mutat* 22: 353–362, 2003.
- Grupe A, Hultgren B, Ryan A, Ma YH, Bauer M, Stewart TA. Transgenic knockouts reveal a critical requirement for pancreatic beta cell glucokinase in maintaining glucose homeostasis. *Cell* 83: 69–78, 1995.
- 21. Gundersen HJ, Bendtsen TF, Korbo L, Marcussen N, Moller A, Nielsen K, Nyengaard JR, Pakkenberg B, Sorensen FB, Vesterby A. Some new, simple and efficient stereological methods and their use in pathological research and diagnosis. APMIS 96: 379–394, 1988.
- Hattersley AT, Pearson ER. Pharmacogenetics and beyond: the interaction of therapeutic response, beta-cell physiology, and genetics in diabetes. *Endocrinology* 147: 2657–2663, 2006.
- 23. Herbach N, Goeke B, Schneider M, Hermanns W, Wolf E, Wanke R. Overexpression of a dominant negative GIP receptor in transgenic mice results in disturbed postnatal pancreatic islet and beta-cell development. Regul Pept 125: 103–117, 2005.
- 24. Herbach N, Rathkolb B, Kemter E, Pichl L, Klaften M, Hrabé de Angelis M, Halban PA, Wolf E, Aigner B, Wanke R. Dominantnegative effects of a novel mutated Ins2 allele causes early-onset diabetes and severe beta-cell loss in Munich *Ins2*<sup>C95S</sup> mutant mice. *Diabetes* 56: 1268–1276, 2007.
- 25. Herbach N, Schairer I, Blutke A, Kautz S, Siebert A, Goke B, Wolf E, Wanke R. Diabetic kidney lesions of GIPR<sup>dn</sup> transgenic mice: podocyte hypertrophy and thickening of the GBM precede glomerular hypertrophy and glomerulosclerosis. *Am J Physiol Renal Physiol* 296: F819–F829, 2009.
- 26. Hrabé de Angelis M, Flaswinkel H, Fuchs H, Rathkolb B, Soewarto D, Marschall S, Heffner S, Pargent W, Wuensch K, Jung M, Reis A, Richter T, Alessandrini F, Jakob T, Fuchs E, Kolb H, Kremmer E, Schaeble K, Rollinski B, Roscher A, Peters C, Meitinger T, Strom T, Steckler T, Holsboer F, Klopstock T, Gekeler F, Schindewolf C, Jung T, Avraham K, Behrendt H, Ring J, Zimmer A, Schughart K, Pfeffer K, Wolf E, Balling R. Genome-wide, large-scale production of mutant mice by ENU mutagenesis. Nat Genet 25: 444–447, 2000.
- 27. Inoue M, Sakuraba Y, Motegi H, Kubota N, Toki H, Matsui J, Toyoda Y, Miwa I, Terauchi Y, Kadowaki T, Shigeyama Y, Kasuga M, Adachi T, Fujimoto N, Matsumoto R, Tsuchihashi K, Kagami T, Inoue A, Kaneda H, Ishijima J, Masuya H, Suzuki T, Wakana S, Gondo Y, Minowa O, Shiroishi T, Noda T. A series of maturity onset diabetes of the young, type 2 (MODY2) mouse models generated by a large-scale ENU mutagenesis program. Hum Mol Genet 13: 1147–1157, 2004.
- Johnson J. Pancreatic beta-cell apoptosis in maturity onset diabetes of the young. Can J Diabetes 31: 67–74, 2007.
- Kauri LM, Wang GS, Patrick C, Bareggi M, Hill DJ, Scott FW. Increased islet neogenesis without increased islet mass precedes autoimmune attack in diabetes-prone rats. *Lab Invest* 87: 1240–1251, 2007.

- 30. **Keays DA, Clark TG, Flint J.** Estimating the number of coding mutations in genotypic- and phenotypic-driven *N*-ethyl-*N*-nitrosourea (ENU) screens. *Mamm Genome* 17: 230–238, 2006.
- Kim WH, Lee JW, Suh YH, Hong SH, Choi JS, Lim JH, Song JH, Gao B, Jung MH. Exposure to chronic high glucose induces beta-cell apoptosis through decreased interaction of glucokinase with mitochondria: downregulation of glucokinase in pancreatic beta-cells. *Diabetes* 54: 2602–2611, 2005.
- 32. Le May C, Chu K, Hu M, Ortega CS, Simpson ER, Korach KS, Tsai MJ, Mauvais-Jarvis F. Estrogens protect pancreatic beta-cells from apoptosis and prevent insulin-deficient diabetes mellitus in mice. *Proc Natl Acad Sci USA* 103: 9232–9237, 2006.
- Louet JF, LeMay C, Mauvais-Jarvis F. Antidiabetic actions of estrogen: insight from human and genetic mouse models. *Curr Atheroscler Rep* 6: 180–185, 2004.
- Matschinsky FM. Glucokinase as glucose sensor and metabolic signal generator in pancreatic beta-cells and hepatocytes. *Diabetes* 39: 647–652, 1990
- Matschinsky FM. Regulation of pancreatic beta-cell glucokinase: from basics to therapeutics. *Diabetes* 51, *Suppl* 3: S394–S404, 2002.
- 36. Matthews DR, Hosker JP, Rudenski AS, Naylor BA, Treacher DF, Turner RC. Homeostasis model assessment: insulin resistance and betacell function from fasting plasma glucose and insulin concentrations in man. *Diabetologia* 28: 412–419, 1985.
- Nielsen JH, Galsgaard ED, Moldrup A, Friedrichsen BN, Billestrup N, Hansen JA, Lee YC, Carlsson C. Regulation of beta-cell mass by hormones and growth factors. *Diabetes* 50, *Suppl* 1: S25–S29, 2001.
- Niswender KD, Postic C, Jetton TL, Bennett BD, Piston DW, Efrat S, Magnuson MA. Cell-specific expression and regulation of a glucokinase gene locus transgene. *J Biol Chem* 272: 22564–22569, 1997.
- 39. Njolstad PR, Sagen JV, Bjorkhaug L, Odili S, Shehadeh N, Bakry D, Sarici SU, Alpay F, Molnes J, Molven A, Sovik O, Matschinsky FM. Permanent neonatal diabetes caused by glucokinase deficiency: inborn error of the glucose-insulin signaling pathway. *Diabetes* 52: 2854–2860, 2003
- 40. Njolstad PR, Sovik O, Cuesta-Munoz A, Bjorkhaug L, Massa O, Barbetti F, Undlien DE, Shiota C, Magnuson MA, Molven A, Matschinsky FM, Bell GI. Neonatal diabetes mellitus due to complete glucokinase deficiency. N Engl J Med 344: 1588–1592, 2001.
- Onishi T, Okawa R, Ogawa T, Shintani S, Ooshima T. Phex mutation causes the reduction of npt2b mRNA in teeth. *J Dent Res* 86: 158–162, 2007
- 42. Osbak KK, Colclough K, Saint-Martin C, Beer NL, Bellanne-Chantelot C, Ellard S, Gloyn AL. Update on mutations in glucokinase (GCK), which cause maturity-onset diabetes of the young, permanent neonatal diabetes, and hyperinsulinemic hypoglycemia. *Hum Mutat* 30: 1512–1526, 2009.
- 43. Pamir N, Lynn FC, Buchan AMJ, Ehses J, Hinke SA, Pospisilik JA, Miyawaki K, Yamada Y, Seino Y, McIntosh CHS, Pederson RA. Glucose-dependent insulinotropic polypeptide receptor null mice exhibit compensatory changes in the enteroinsular axis. Am J Physiol Endocrinol Metab 284: E931–E939, 2003.
- 44. Paris M, Bernard-Kargar C, Berthault MF, Bouwens L, Ktorza A. Specific and combined effects of insulin and glucose on functional pancreatic beta-cell mass in vivo in adult rats. *Endocrinology* 144: 2717– 2727, 2003.
- 45. Paris M, Tourrel-Cuzin C, Plachot C, Ktorza A. Pancreatic beta-cell neogenesis revisited. *Exp Diabesity Res* 5: 111–121, 2004.
- Postic C, Shiota M, Magnuson MA. Cell-specific roles of glucokinase in glucose homeostasis. *Recent Prog Horm Res* 56: 195–217, 2001.
- 47. Postic C, Shiota M, Niswender KD, Jetton TL, Chen Y, Moates JM, Shelton KD, Lindner J, Cherrington AD, Magnuson MA. Dual roles for glucokinase in glucose homeostasis as determined by liver and pancreatic beta cell-specific gene knock-outs using Cre recombinase. *J Biol Chem* 274: 305–315, 1999.
- 48. **Rabinovitch A, Quigley C, Russell T, Patel Y, Mintz DH.** Insulin and multiplication stimulating activity (an insulin-like growth factor) stimulate islet beta-cell replication in neonatal rat pancreatic monolayer cultures. *Diabetes* 31: 160–164, 1982.
- 49. Rathkolb B, Decker T, Fuchs E, Soewarto D, Fella C, Heffner S, Pargent W, Wanke R, Balling R, Hrabé de Angelis M, Kolb HJ, Wolf E. The clinical-chemical screen in the Munich ENU Mouse Mutagenesis Project: screening for clinically relevant phenotypes. *Mamm Genome* 11: 543–546, 2000.

- Rathkolb B, Fuchs E, Kolb HJ, Renner-Muller I, Krebs O, Balling R, Hrabé de Angelis M, Wolf E. Large-scale N-ethyl-N-nitrosourea mutagenesis of mice—from phenotypes to genes. Exp Physiol 85: 635–644, 2000
- Rohrl J, Yang D, Oppenheim JJ, Hehlgans T. Identification and biological characterization of mouse beta-defensin 14, the orthologue of human beta-defensin 3. *J Biol Chem* 283: 5414–5419, 2008.
- 52. Sagen JV, Odili S, Bjorkhaug L, Zelent D, Buettger C, Kwagh J, Stanley C, Dahl-Jorgensen K, de Beaufort C, Bell GI, Han Y, Grimsby J, Taub R, Molven A, Sovik O, Njolstad PR, Matschinsky FM. From clinicogenetic studies of maturity-onset diabetes of the young to unraveling complex mechanisms of glucokinase regulation. *Diabetes* 55: 1713–1722, 2006.
- Schuppin GT, Bonner-Weir S, Montana E, Kaiser N, Weir GC. Replication of adult pancreatic-beta cells cultured on bovine corneal endothelial cell extracellular matrix. *In Vitro Cell Dev Biol Anim* 29A: 339–344, 1993.
- 54. Sreenan SK, Cockburn BN, Baldwin AC, Ostrega DM, Levisetti M, Grupe A, Bell GI, Stewart TA, Roe MW, Polonsky KS. Adaptation to hyperglycemia enhances insulin secretion in glucokinase mutant mice. *Diabetes* 47: 1881–1888, 1998.
- 55. Terauchi Y, Sakura H, Yasuda K, Iwamoto K, Takahashi N, Ito K, Kasai H, Suzuki H, Ueda O, Kamada N, Kouichi Jishage K, Komeda K, Noda M, Kanazawa Y, Taniguchi S, Miwa I, Akanuma Y, Kodama T, Yazaki Y, Kadowaki T. Pancreatic beta-cell-specific targeted disruption of glucokinase gene. Diabetes mellitus due to defective insulin secretion to glucose. *J Biol Chem* 270: 30253–30256, 1995.
- 56. Terauchi Y, Takamoto I, Kubota N, Matsui J, Suzuki R, Komeda K, Hara A, Toyoda Y, Miwa I, Aizawa S, Tsutsumi S, Tsubamoto Y, Hashimoto S, Eto K, Nakamura A, Noda M, Tobe K, Aburatani H,

- **Nagai R, Kadowaki T.** Glucokinase and IRS-2 are required for compensatory beta cell hyperplasia in response to high-fat diet-induced insulin resistance. *J Clin Invest* 117: 246–257, 2007.
- 57. Toye AA, Moir L, Hugill A, Bentley L, Quarterman J, Mijat V, Hough T, Goldsworthy M, Haynes A, Hunter AJ, Browne M, Spurr N, Cox RD. A new mouse model of type 2 diabetes, produced by *N*-ethylnitrosourea mutagenesis, is the result of a missense mutation in the glucokinase gene. *Diabetes* 53: 1577–1583, 2004.
- Trus MD, Zawalich WS, Burch PT, Berner DK, Weill VA, Matschinsky FM. Regulation of glucose metabolism in pancreatic islets. *Diabetes* 30: 911–922, 1981.
- 59. van de Bunt M, Gloyn AL. Monogenic disorders of the pancreatic β-cell: personalizing treatment for rare forms of diabetes and hypoglycemia. Personalized Med 4: 247–259, 2007.
- 60. Velho G, Blanche H, Vaxillaire M, Bellanne-Chantelot C, Pardini VC, Timsit J, Passa P, Deschamps I, Robert JJ, Weber IT, Marotta D, Pilkis SJ, Lipkind GM, Bell GI, Froguel P. Identification of 14 new glucokinase mutations and description of the clinical profile of 42 MODY-2 families. *Diabetologia* 40: 217–224, 1997.
- Velho G, Froguel P. Genetic, metabolic and clinical characteristics of maturity onset diabetes of the young. Eur J Endocrinol 138: 233–239, 1998
- Velho G, Vaxillaire M, Boccio V, Charpentier G, Froguel P. Diabetes complications in NIDDM kindreds linked to the MODY3 locus on chromosome 12q. *Diabetes Care* 19: 915–919, 1996.
- Wallace TM, Levy JC, Matthews DR. Use and abuse of HOMA modeling. *Diabetes Care* 27: 1487–1495, 2004.
- 64. Wanke RWS, Kluge D, Kahnt E, Schenck E, Brem G, Herrmanns W. Morphometric evaluation of the pancreas of growth hormone-transgenic mice. Acta Stereol 3–8, 1994.

